SUPPORTING INFORMATION

EBT anchored SiO2 3-D microarray: A simultaneous entrapper of two different metal centers at High and Low oxidation states using its respective highest occupied and lowest unoccupied molecular orbital

Bhavya Srivastava, Milan K. Barman, Mousumi Chatterjee and Bhabatosh Mandal*

Analytical Laboratory, Department of Chemistry,

Visva-Bharati, Santiniketan 731235, India

*Author to whom all correspondence should be addressed: E-mail: bhabatosh_mandal@yahoo.co.in

Mobile No: + (91)9474738517

Schemes:

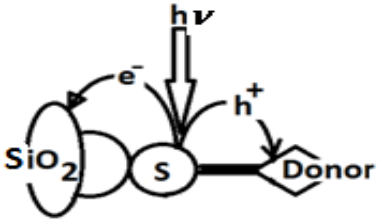

Scheme S1

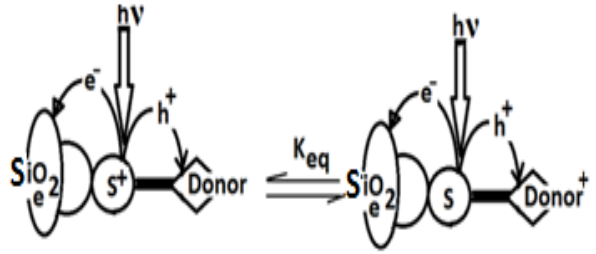

Scheme S2

File S1:

The specific surface area was calculated by the Brunauer-Emmett-Teller (BET) method using the adsorption branch.

BET (Specific Surface Area) Result: (t-Plot external surface area: 339.8254 $m^2 g^{-1}$; Single point surface area at P / P_0 of 0.300006229: 317.8206 $m^2 g^{-1}$; BJH adsorption cumulative surface area of pores between 17.0 A - 3000.0 A diameter: 324.381 $m^2 g^{-1}$; BJH desorption cumulative surface area of pores between 17.0 A - 3000.0 A diameter: 364.511 $m^2 g^{-1}$ and pore volumes (single point adsorption total pore volume of pores less than 1014.164 A diameter at P/P_0 of 0.980530216: 0.388974 $cm^3 g^{-1}$; t-Plot micro pore volume: -0.007751 $cm^3 g^{-1}$; BJH adsorption cumulative volume of pores between 17.0 A - 3000.0 A diameter: 0.374689 $cm^3 g^{-1}$; BJH desorption cumulative volume of pores between 17.0 A - 3000.0 A diameter: 0.418756 $cm^3 g^{-1}$) of the dry exchanger were obtained by BET analysis (Fig. 3c) and emphasizes the analytical application of the synthesized material. It also gives the pore sizes: 47.0107 A and 46.204 A respectively for the adsorption average pore width (4V/A by BET) and BJH adsorption average pore diameter (4V/A)).

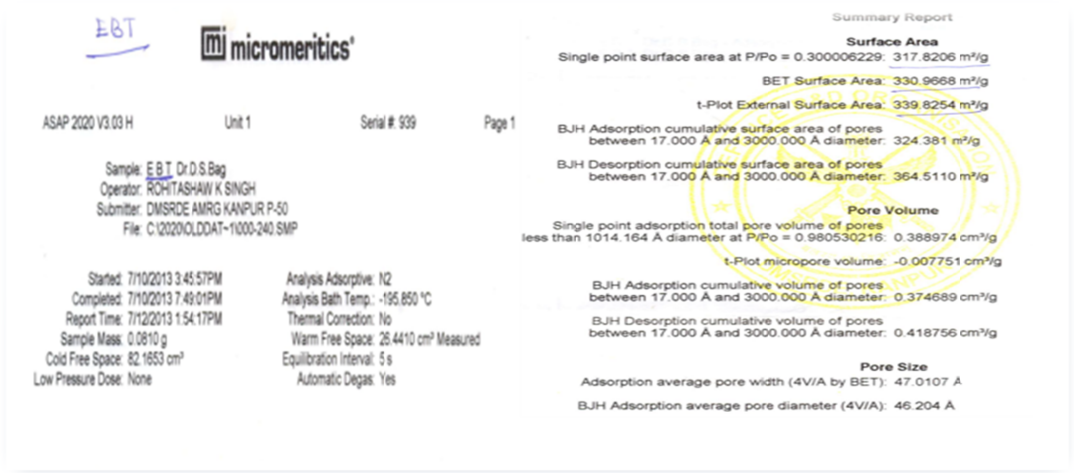
EBT

micromeritics

ASAP 2020 V3.03 H Unit 1 Serial #: 939 Page 1

Sample: E B T Dr.D.S.Bag
Operator: ROHITASHAW K SINGH
Submitter: DMSRDE AMRG KANPUR P-50
File: C:\2020\OLDDAT~1\000-240.SMP

Started: 7/10/2013 3:45:57PM
Completed: 7/10/2013 7:49:01PM
Report Time: 7/12/2013 1:54:17PM
Sample Mass: 0.0810 g
Cold Free Space: 82.1653 cm³
Low Pressure Dose: None

Analysis Adsorptive: N2
Analysis Bath Temp.: -195.850 °C
Thermal Correction: No
Warm Free Space: 26.4410 cm³ Measured
Equilibration Interval: 5 s
Automatic Degas: Yes

Summary Report

Surface Area

Single point surface area at P/Po = 0.300006229: 317.8206 m²/g
BET Surface Area: 330.9668 m²/g
t-Plot External Surface Area: 339.8254 m²/g
BJH Adsorption cumulative surface area of pores between 17.000 Å and 3000.000 Å diameter: 324.381 m²/g
BJH Desorption cumulative surface area of pores between 17.000 Å and 3000.000 Å diameter: 364.5110 m²/g

Pore Volume

Single point adsorption total pore volume of pores less than 1014.164 Å diameter at P/Po = 0.980530216: 0.388974 cm³/g
t-Plot micropore volume: -0.007751 cm³/g
BJH Adsorption cumulative volume of pores between 17.000 Å and 3000.000 Å diameter: 0.374689 cm³/g
BJH Desorption cumulative volume of pores between 17.000 Å and 3000.000 Å diameter: 0.418756 cm³/g

Pore Size

Adsorption average pore width (4V/A by BET): 47.0107 Å
BJH Adsorption average pore diameter (4V/A): 46.204 Å

Scheme S3: Synthesis of the extractor: Chemical structure of Resin (FSG-EBT)

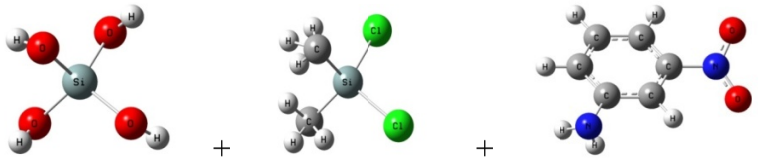

A + C + B

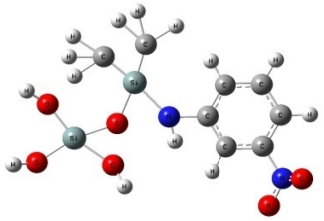

D

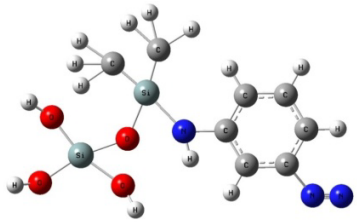

E (diazo-compund)

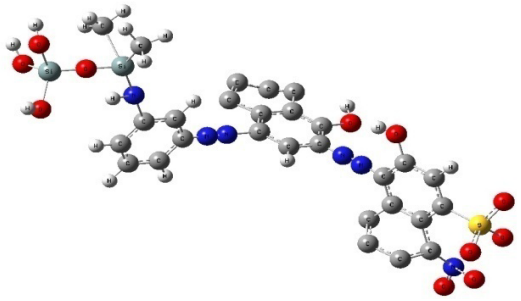

F (Resin: Diazo-EBT complex)

Scheme-S3 (synthesis of the resin)

Table S1: Selected experimental FT-IR and RAMAN bands of extractor (FSG-EBT) and B3LYP/6-STO-3G (d) calculated vibration modes with considerable Raman intensity.

RAMAN (Exp.) (cm^{-1}) FT-IR(Exp.) (cm^{-1})	**B3LYP (DFT) (cm^{-1})**	**RAMAN / FTIR [50,51] (Reported) (cm^{-1})**	**Band Assignment**
(1065, 1088)$^{a+}$(1203)$^{b-}$ (420,710,820)^{c}	(781, 1070)$^{a+}$ (1230)$^{b-}$ (450,705,840)^{c}	(1075)$^{a+}$(1201,1232)$^{b-}$ (414,470,764,810)^{c}	Si-O-Si linkage [10]
(900-1203)$^{b+}$ (1100)$^{b-}$	(850-1100)$^{b+}$ (1120)$^{b-}$	(950-1200)$^{b+}$ (1080-1100)$^{b-}$	Si-O[11a]
(2192)$^{a+}$ (2270)$^{b-}$	(2000)$^{a+}$ (2150)$^{b-}$	(2187)$^{a+}$ (2170)$^{b-}$	Si–H[11b]
(1518, 1595)$^{a+}$ (1320)$^{b-}$ (1422, 1559)$^{b+}$	(1500,1600)$^{a-}$ (1570)$^{b-}$ (1450)$^{b+}$	(1505,1594)$^{a+}$ (1614)$^{a-}$ (1576)$^{b-}$ (1565, 1617)$^{b+}$	-NO_2
(1136)$^{a+}$ (1107,1559)$^{b+}$ (1120)$^{b-}$	(1130)$^{a+}$ (1100,1550)$^{b-}$ (1125)$^{b+}$	(1130)$^{a+}$ (1144,1540)$^{b+}$ (1145)$^{b-}$	-S=O & -OH in –SO_3H (Silanol group)
(1281-1372)$^{a+}$(1516-1570)$^{a-}$(1559)$^{b-}$(1320)$^{b+}$	(1281-1372)$^{a+}$(1500-1580)$^{a-}$(1559)$^{b-}$ (1350)$^{b+}$	(1293-1374)$^{a+}$ (1505-1594)$^{a-}$ (1501-1617)$^{b-}$ (1397)$^{b+}$	-C-C-stretching of pyridine ring
(1518)$^{a+}$ (951,2031)$^{b-}$ (1320)^{c}	(1500)$^{a+}$ (800,2010)$^{b+}$ (1350)^{c}	(1505-1558)$^{a+}$ (884,2089,2123)$^{b-}$(1335)^{c}	-N=N-stretching[12], amidst (i) EBT,EBT- diazotized FSG
(1450-1480)$^{a+}$ (1200)$^{b-}$	(1400, 1435)$^{a+}$ (1250)$^{b-}$	(1447-1470)$^{a+}$ (1274)$^{b-}$	ϕ C-H stretching of pyridine ring.

(1136)$^{a+}$(1050,1107)$^{b-}$ (807)^{c}	(1160)$^{a+}$(1050;1120)$^{b-}$ (830)^{c}	(1144)$^{a+}$ (1049,1145)$^{b-}$ (803)^{c}	O-H in SO_3H
(3300)$^{a+}$ (3525) $^{b--}$ (1120)^{c}	(3400)$^{a+}$ (3540.51)$^{b--}$ (1170)^{c}	(3350)$^{a+}$ (3100-3500)$^{b-}$ (1175)^{c}	N-H in (Si-N(H)-C(ϕ-ring))
(1137-1559)$^{a+}$(1050-1559)^{c}	(1110-1570)$^{a+}$(1049-1650)^{c}	(1144-1558)$^{a+}$ (1049-1617)^{c}	Phenolic-OH of naphthol
((1137-1559)$^{a+}$ (816,1150-1559)$^{b-}$	(1100-1570)$^{a+}$ (840,1100-1595)$^{b-}$	(1144-1558)$^{a+}$(803,1049-1617)$^{b-}$	O-H in $Si(OH)_3$
(1050,1233,1291,1336) $^{a+}$ (2350)$^{b-}$	(1054,1245,1360)$^{a+}$ (2200)$^{b-}$	(1047, 1240, 1293, 1335)$^{a+}$ (2200)$^{b-}$	C-N linkage [13]
(858-1203)$^{b-}$	(850-1180)$^{b-}$	(862-1170)$^{b-}$	Si-N stretching [14]
(978,1012-1614)$^{a+}$ (3697)$^{b-}$ (951-1632)^{c}	(1017-1620)$^{a+}$(3600)$^{b+}$ (1050-1559)^{c}	(973,1007-1614)$^{a+}$(3655-3699)$^{b-}$ (1047-1594)^{c}	C-H of aliphatic CH_3 attached to Si [15]

a = Raman; b = FT-IR; c = bending; -ve = sym. Stretching; +ve = assym. Stretching; ϕ = aromatic

Figure S1: Experimental Raman spectra (Experimental Raman Spectra (upper curve corresponds to the Th-loaded exchanger while lower curve corresponds to the unloaded exchanger))

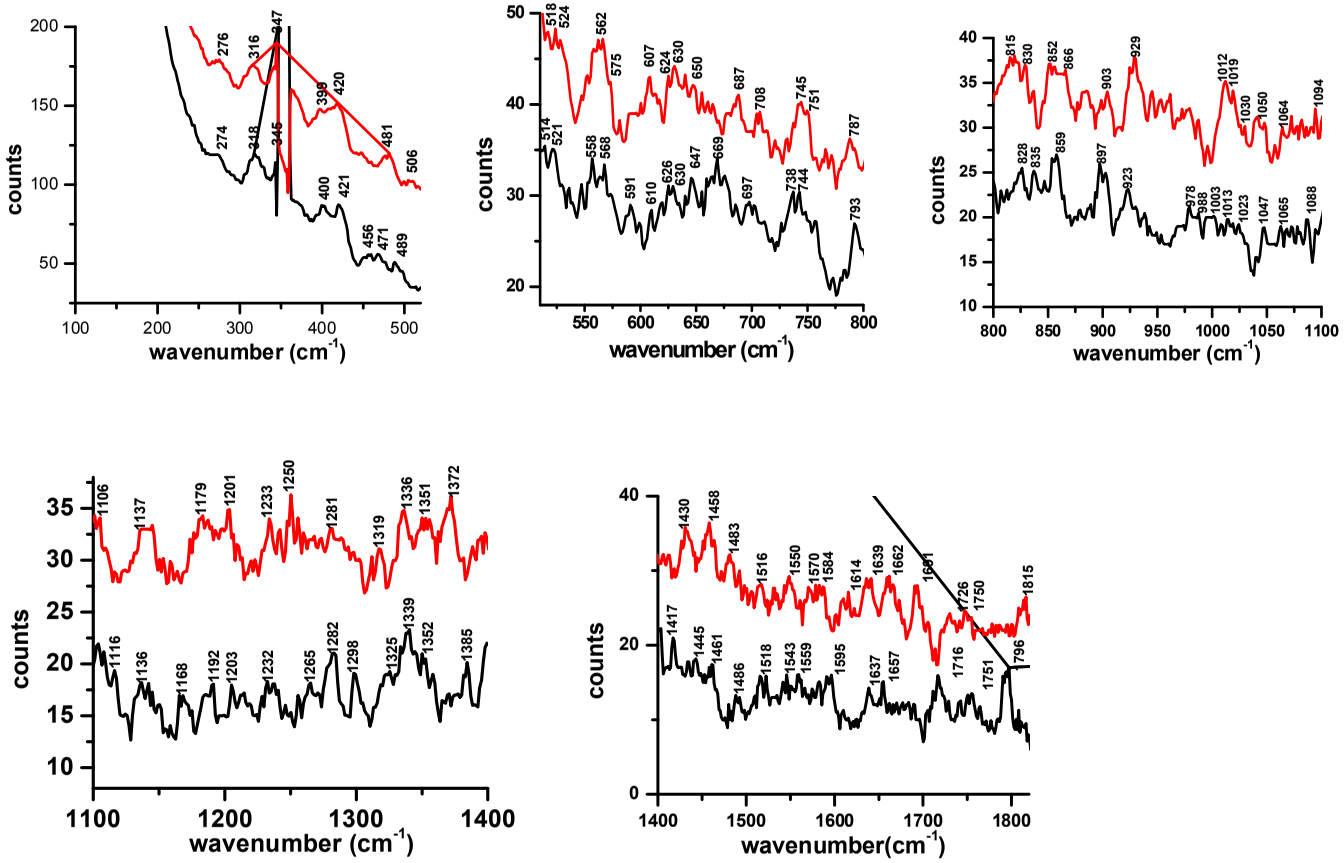

Figure S2: DFT calculated NMR spectra of ^{1}H (a) and ^{13}C NMR (b) of a model compound (c) comprising one tetrahedral edge of FSG-EBT used in DFT calculation for NMR spectra.

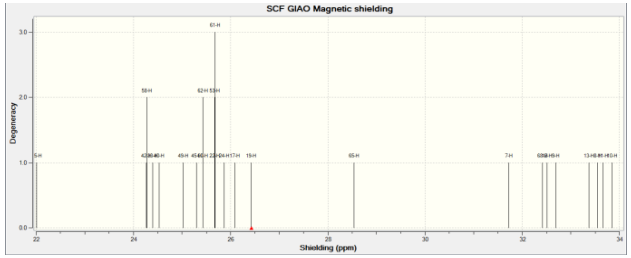

(a)

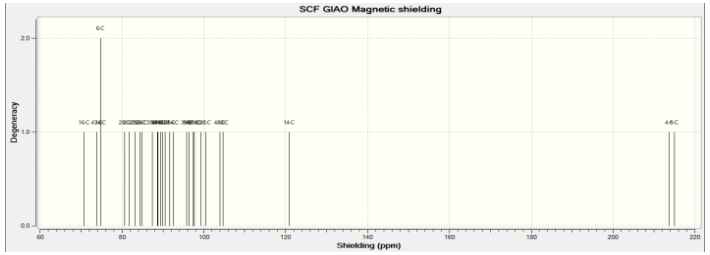

(b)

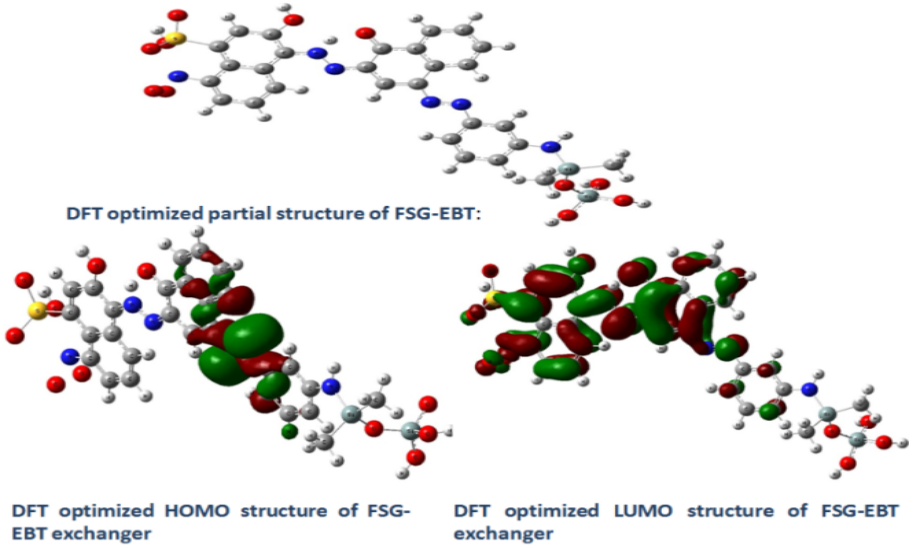

(c)

[Considering the symmetry properties of the molecule only one tetrahedral edge of FSG-EBT was taken as a model compound (Figure S2 c) to have the NMR spectra from DFT calculation. In the DFT NMR spectra (Figure S2 (a-b)) there are six pair of aromatic carbons of similar δ (ppm) values in its ^{13}C spectrum [84.8986 and 84.4461 for (C52 & C26); 74.7593 and 74.7813 for (C34 & C6); 88.6252 and 88.7531 for (C59 & C41); 97.3881 and 97.7202 for (C57 & C15); 89.3824 and 89.8880 for (C46 & C18); 95.7599 and 96.4242 for (C39 & C56)] suggesting the shortage of 6 aromatic carbons in experimental spectra (^{13}C NMR) and clearly confirms the molecular structure

of FSG-EBT (Figure 5b). However, the probable spin restriction for the presence of metal ions, the loaded extractor generates no characteristic NMR signals. Rather a single broad peak, merged with solvent signal appears in the spectrum.]

Figure S3: (a) experimental ^{1}H NMR spectra of FSG (b) experimental ^{13}C NMR spectra of FSG; (c) experimental ^{1}H NMR of FSG-EBT (d) experimental ^{13}C NMR of FSG-EBT

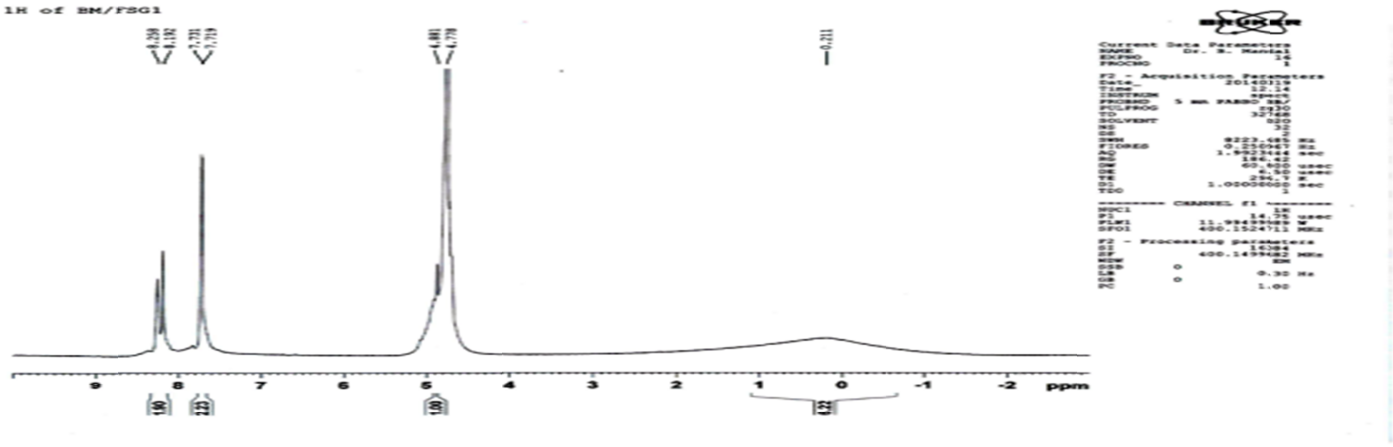

(a)

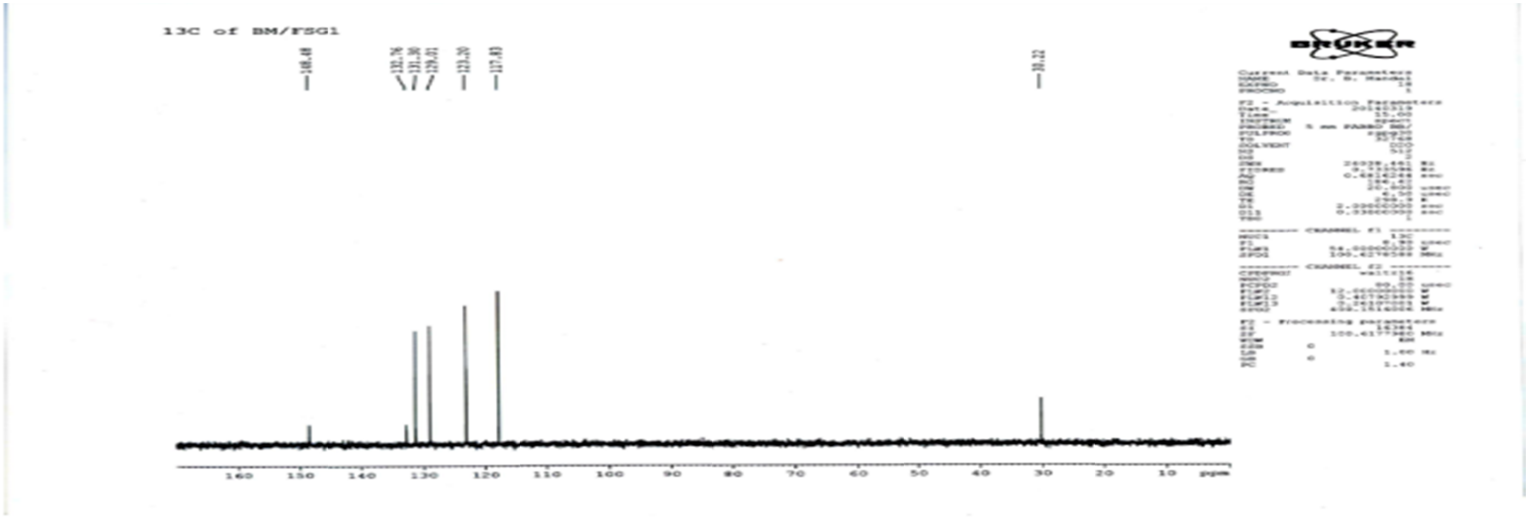
13C of BM/FSG1
160.48
132.76
131.36
129.01
123.30
117.83
29.22
160
150
140
130
120
110
100
90
80
70
60
50
40
30
20
10
ppm

(b)

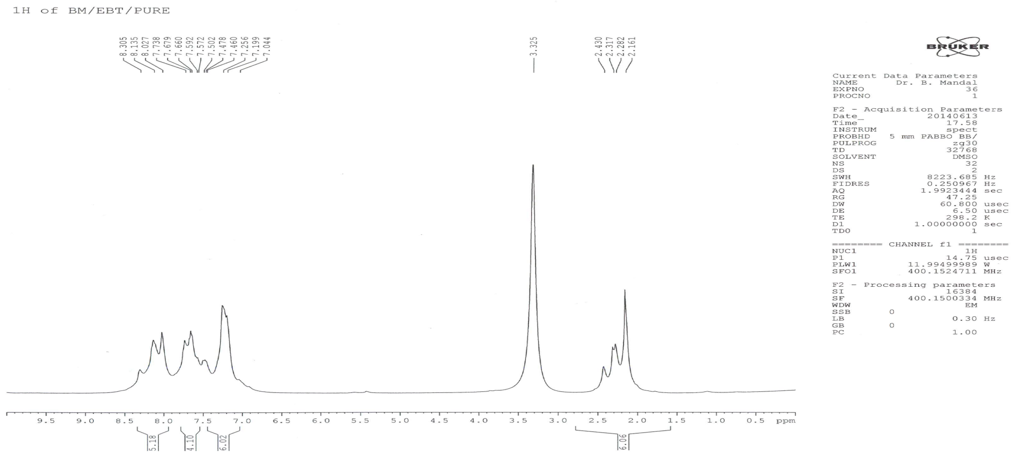
1H of BM/EBT/PURE
8.305 8.135 8.027 7.738 7.679 7.660 7.592 7.572 7.502 7.478 7.460 7.256 7.199 7.044
3.325
2.430 2.317 2.282 2.161
5.18 4.10 6.02 6.06
ppm
Current Data Parameters
NAME Dr. B. Mandal
EXPNO 36
PROCNO 1
F2 - Acquisition Parameters
Date_ 20140613
Time 17.58
INSTRUM spect
PROBHD 5 mm PABBO BB/
PULPROG zg30
TD 32768
SOLVENT DMSO
NS 32
DS 2
SWH 8223.685 Hz
FIDRES 0.250967 Hz
AQ 1.9923444 sec
RG 47.25
DW 60.800 usec
DE 6.50 usec
TE 298.2 K
D1 1.00000000 sec
TD0 1
CHANNEL f1
NUC1 1H
P1 14.75 usec
PLW1 11.99499989 W
SFO1 400.1524711 MHz
F2 - Processing parameters
SI 16384
SF 400.1500334 MHz
WDW EM
SSB 0
LB 0.30 Hz
GB 0
PC 1.00

(c)

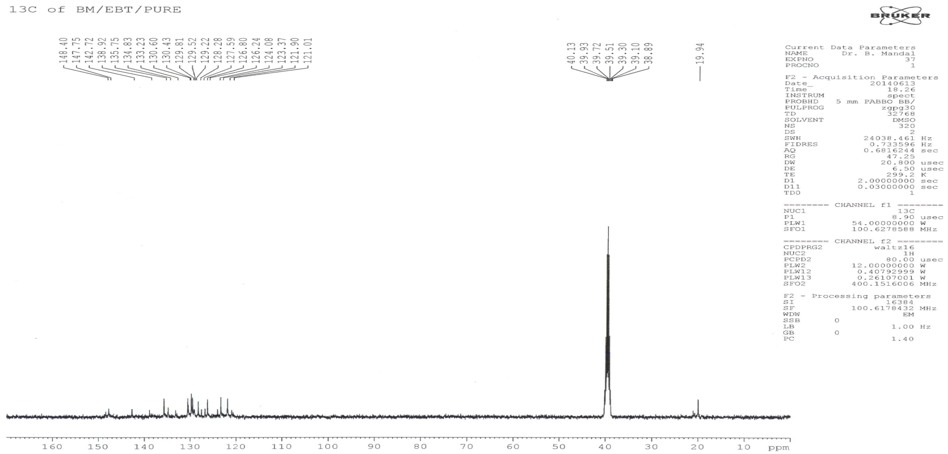
13C of BM/EBT/PURE
148.40 147.75 142.72 138.92 135.75 134.83 133.23 130.60 130.43 129.81 129.52 129.22 128.28 127.59 126.80 126.24 124.08 123.37 121.90 121.01
40.13 39.93 39.72 39.51 39.30 39.10 38.89
19.94
ppm
Current Data Parameters
NAME Dr. B. Mandal
EXPNO 37
PROCNO 1
F2 - Acquisition Parameters
Date_ 20140613
Time 18.26
INSTRUM spect
PROBHD 5 mm PABBO BB/
PULPROG zgpg30
TD 32768
SOLVENT DMSO
NS 320
DS 2
SWH 24038.461 Hz
FIDRES 0.733596 Hz
AQ 0.6816244 sec
RG 47.25
DW 20.800 usec
DE 6.50 usec
TE 299.2 K
D1 2.00000000 sec
D11 0.03000000 sec
TD0 1
CHANNEL f1
NUC1 13C
P1 8.90 usec
PLW1 54.00000000 W
SFO1 100.6278588 MHz
CHANNEL f2
CPDPRG2 waltz16
NUC2 1H
PCPD2 80.00 usec
PLW2 12.00000000 W
PLW12 0.40792999 W
PLW13 0.26107001 W
SFO2 400.1516006 MHz
F2 - Processing parameters
SI 16384
SF 100.6178432 MHz
WDW EM
SSB 0
LB 1.00 Hz
GB 0
PC 1.40

(d)

Figure S4: TD-DFT UV-Vis spectra of FSG-EBT

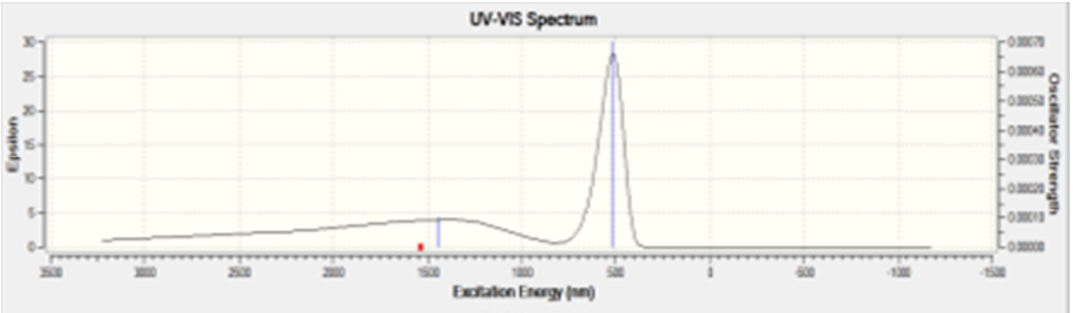

Figure S5: (a-i) DFT optimized structures of the relevant building units of the resin

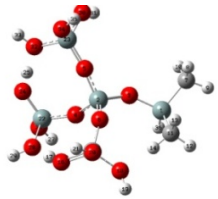

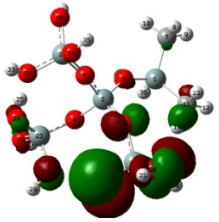

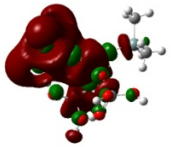

(a) Silica gel-DMDCS composite HOMO (-6.96617 eV) LUMO (-1.68712 eV) (-2502.3532 au; η= 5.27905 eV)

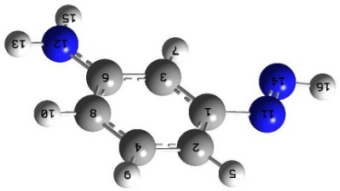

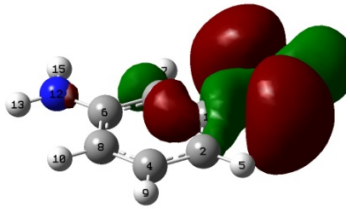

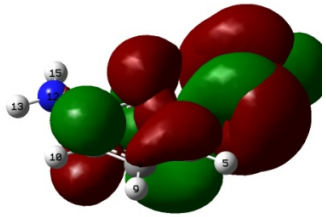

(b) Nitro aniline (-394.8002 au; η = 1.74154 eV) HOMO (-5.1974156 eV) LUMO (-3.4558732 eV)

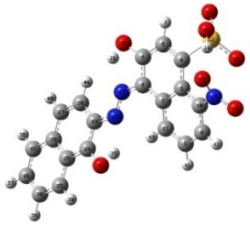

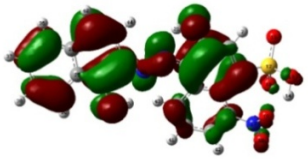

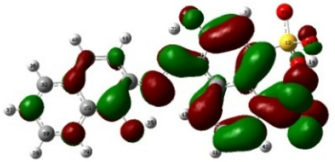

(c) EBT (-1849.6413au; η = 1.1701 eV) HOMO (-6.476361 eV) LUMO (-5.306262 eV)

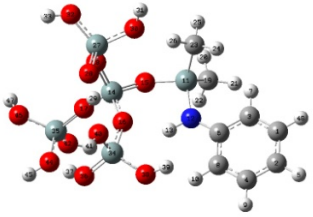
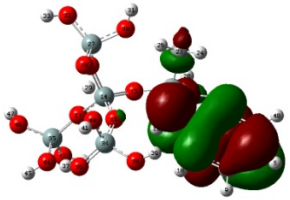
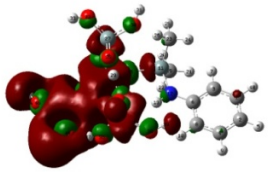

(d) SG-DMDCS-aniline (-2787.15324 au; η = 3.183757 eV) HOMO (-5.0885692 eV) LUMO (-1.9048120 eV)

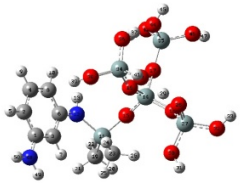
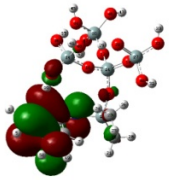


(e) Silica-DMDCS-m-aminoaniline (-2842.2366 au; η = 3.5919312 eV) HOMO (-5.2246272 eV) LUMO(-1.632696 eV)

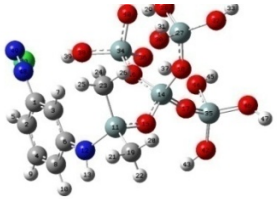
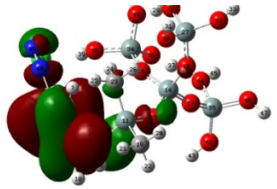
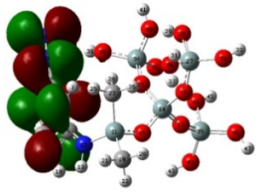

(f) Silica–DMDCS- m-aminoaniline-chloride (3354.4602 au; η =1.98643 eV) HOMO (-6.1770332 eV); LUMO (-4.1906 eV)

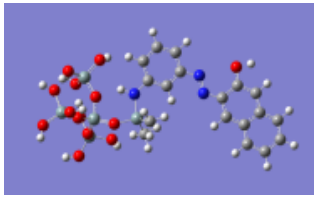

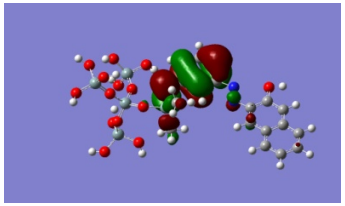

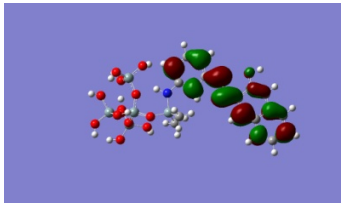

(g) Silica-m-diazonaph-aniline (η = 1.7252 eV) HOMO (-5.2319 eV) LUMO (3.5068 eV)

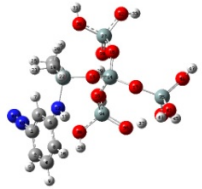

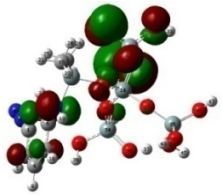

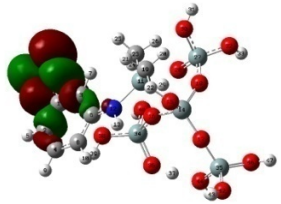

(h): Chloride salt of (g) (-3936.4161 a.u.; η =2.5842) HOMO (-9.3063672 eV) LUMO (-8.571654 eV)

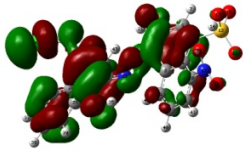

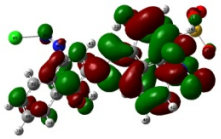

(i) EBT diazo HOMO (-6.8573 eV) LUMO (-5.6872 eV)

(-2416.92 au; 11.06 Debye)

[In all the building moieties viz. SG, linker (m-diazoaniline) and azo-dye (EBT) HOMO-LUMO are not well separated (Figure S5 (a-d)). However, in course of their attachment, HOMO resides at the linker site at every occasion whereas LUMO gradually shifts its position from silanized silica part to the dye component (Figure S5 (d-i)) and finally in the synthesized resin HOMO-LUMO get well separated (Figure 6a-d). Thus, both charge and hole are transferred through a 'quasi-equilibrium' [60] as per Scheme-s1, and suggests the longer life time of the ejected electron placed at the SiO_2 moiety. The expected charge transfer from the different components of the material produce spectral lines at the UV-Vis range (3.5919(348.0); 3.1837(392.6); 1.9864(629.3); 1.4967(835.2 nm) and 1.0701 eV (1168.1 nm)) corresponding to their HOMO-LUMO band gap (Figure S4). The experimental spectral positions (274, 366.4, 450, 578, 880.5, 950.3 and 1094.5 nm) (Figure 7a-b) are nearly compatible and support the transfer of hole by *hopping mechanism*. The privileges, thus highlighted, along with the intra-molecular charge/hole transfer can be exploited for its utility as a LED source.]

Figure S6: Sorption isotherms:

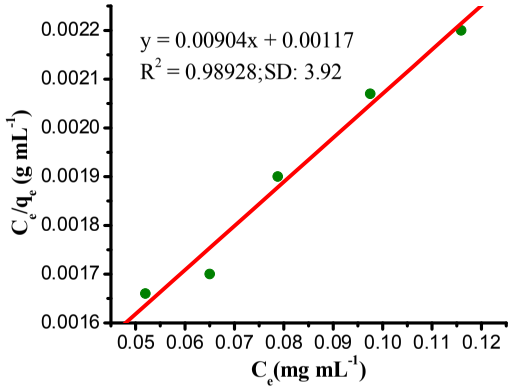

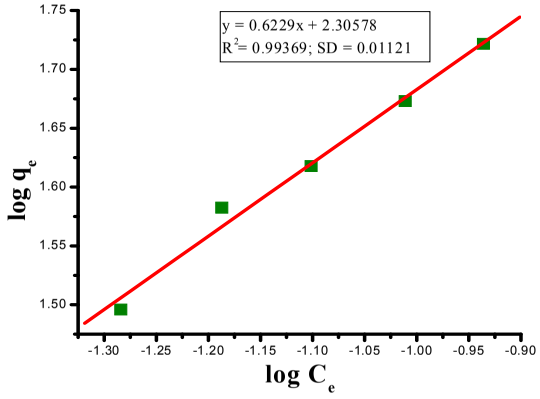

(a) (b)

(a) Plot of C_e (mg mL^{-1}) vs. C_e/q_e ($g\ \ mL^{-1}$) for Langmuir isotherm (b) plot of $\log C_e(\mu mol\ \ mL^{-1})$ vs. $\log q_e(\mu mol\ g^{-1})$ for Freundlich isotherm ($\log q_e = \log K_F + \frac{1}{n}\log C_e$; $K_F = 1.25\times10^2$ and n = 1.61)

Table S2: Langmuir and Freundlich parameters

Langmuir parameters ; R^2 = 0.9893						**Freundlich parameters; R^2 = 0.9936**			
C_e	q_e	Q_0 (mg g^{-1})	b (L mg^{-1})	$q_{e(t)}$	RMSE	$\frac{1}{n}$	k_F	$q_{e(t)}$	RMSE
0.052	31.3253	110.6195	7.7265	31.7057	0.8857	0.623	2.02×10^2	32.0614	0.9636
0.0650	38.2853	476.7 (µM g^{-1})		36.9822				36.8424	
0.0788	41.4737			41.8625				41.6635	
0.0975	47.1015			47.5285				47.4279	
0.1159	52.6818			52.2605				52.8204	

Figure S7: Elution profile of Th (IV)

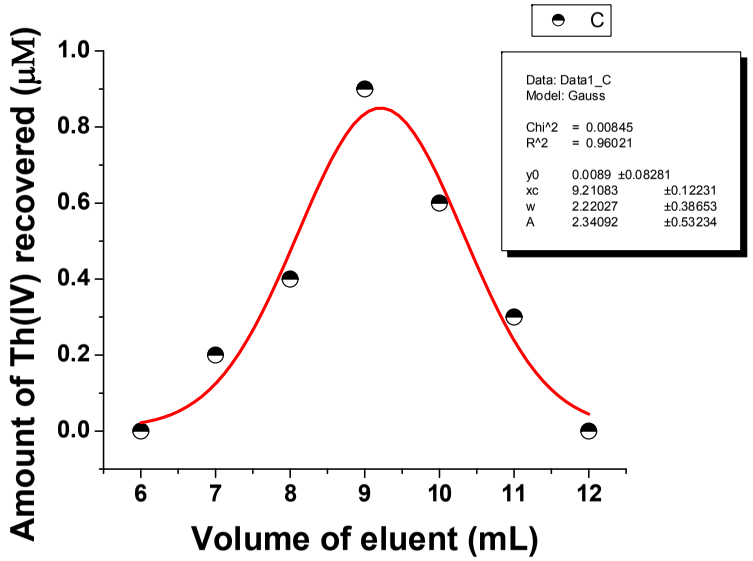

[0.5mol L^{-1} $HClO_4$; total volume: 5 mL; Peak height: 0.84124]

Plate number, $N = 4\times[\frac{y^2}{x^2}] = 296$; Where, $x = \frac{1}{2}\times w_{0.6065\times h}$; $w_{0.6065\times h}$ = width at a 0.6065 times of peak height; y = distance for peak elution.